Scalable Arrays of 107 Gbit/s Surface-Normal Electroabsorption Modulators

Stefano Grillanda[1,*], Ting-Chen Hu[1], David Neilson[2], Nagesh Basavanhally[1], Yee Low[1], Hugo Safar[1], Mark Cappuzzo[1], Rose Kopf[1], Alaric Tate[1], Gregory Raybon[2], Andrew Adamiecki[2], Nicolas Fontaine[2], and Mark Earnshaw[1]

[1]Bell Laboratories, Nokia, 600 Mountain Avenue, Murray Hill, NJ 07974, USA
[2]Bell Laboratories, Nokia, 791 Holmdel-Keyport Road, Holmdel, NJ 07733, USA
*stefano.grillanda@nokia-bell-labs.com

Abstract: We demonstrate arrays of surface-normal electroabsorption modulators with ultrawide bandwidth (>>65 GHz), polarization insensitive response and ultralow total coupling loss to single-mode-fibers (0.7 dB). We show modulation up to 107 Gbit/s and packaging with arrayed-waveguide-gratings.

1. Introduction

Optical modulators are fundamental components of communication systems enabling the transmission of high-speed signals on optical fibers. For instance, complex Mach-Zehnder modulators [1] are typically used in long-haul coherent systems to generate multi-level, dual-polarization, in-phase and in-quadrature signals with high extinction ratio (ER) and no chirp. Short reach systems, such as datacenters and access networks, require instead different types of modulators, with simple structure, low power consumption and small size. For example, silicon (Si) microring resonators enable compact modulators (5-10 μm radius) with low drive voltage (1-2 V_{pp}) [2]. However, the high-quality factor (Q) cavity of microrings (10^3-10^4) limits their electro-optic bandwidth (with records of <50 GHz), and is responsible for the need of stringent wavelength and temperature control (sub-degree). Furthermore, as they are based on Si waveguides, they require complex polarization management circuits to control the polarization of the input light. Here, we demonstrate large scale arrays of polarization insensitive, surface-normal electroabsorption modulators (SNEAMs). By using a low-Q Fabry Perot cavity and the strong quantum confined Stark effect (QCSE) we overcome some of the limitations of microrings. In particular, we show broad wavelength range of modulation without accurate temperature control and ultrawide bandwidth (>>65 GHz). We demonstrate 107 Gbit/s NRZ-OOK modulation and integration of SNEAM arrays with arrayed-waveguide-gratings (AWGs).

2. Single-channel SNEAMs

Figures 1(a-b) show, respectively, a cross-sectional schematic and a top-view photograph of a SNEAM in reflective configuration. SNEAMs are made by an InGaAs/InAlAs multi-quantum-well (MQW) stack placed in the intrinsic region of a p-i-n structure. The MQW is surrounded by a Fabry-Perot cavity formed by a partially-reflective top mirror and a highly-reflective bottom mirror [Fig. 1(a)]. The SNEAM structure is flip-chipped on a submount with

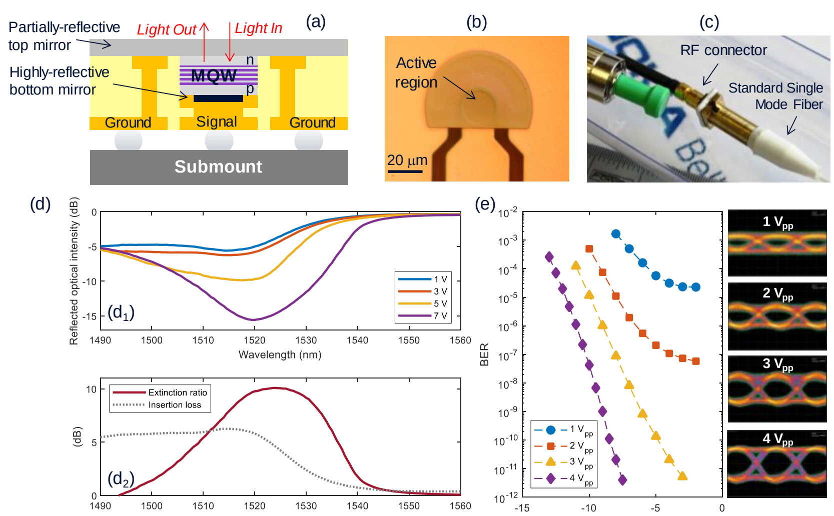

Fig. 1: (a) Cross-sectional schematic, (b) top-view photograph and (c) packaging of a SNEAM. (d_1) Reflected optical intensity of a SNEAM at different reverse bias voltage and (d_2) trade-off between ER and insertion loss when the reverse bias is switched between 3 V and 7 V. (e) Modulation experiments at 25 Gbit/s NRZ-OOK.

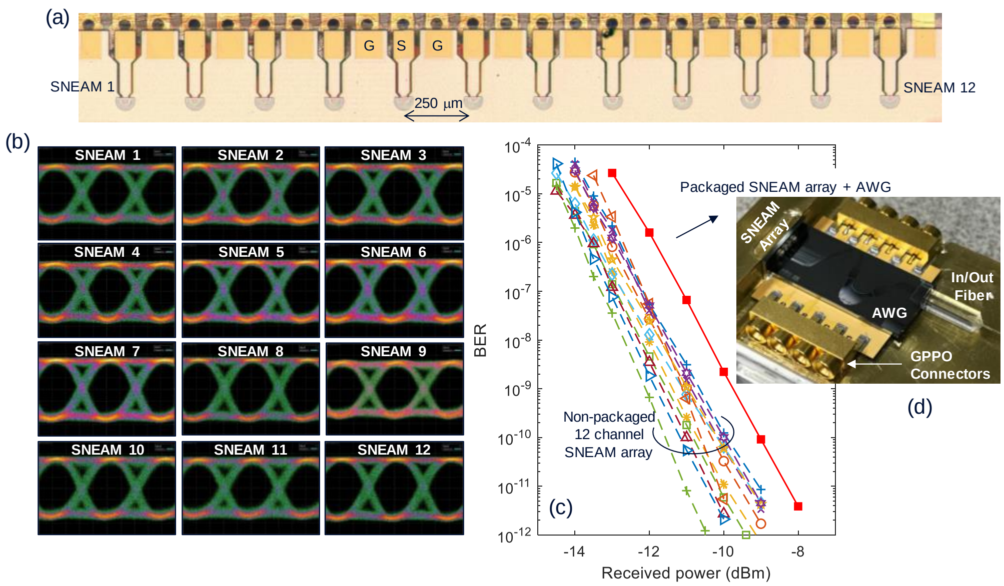

Fig. 2: (a) Top-view photograph of a SNEAM array. (b) Eye diagrams and (c) BER curves of the 12 SNEAMs of the array at 25 Gbit/s NRZ-OOK. Red line and square markers show the BER of one of the channels of the SNEAM array packaged with an AWG to form a WDM transmitter (d).

electrical lines. Figure 1(c) shows the photograph of a SNEAM packaged with a standard single mode fiber and an electrical GPPO radio-frequency (RF) connector. Figures 1(d_1-d_2) show the optical intensity reflected by a SNEAM as a function of wavelength for different reverse bias voltages and the trade-off between ER and insertion loss when the reverse bias voltage is switched between 3 V and 7 V. Under application of a reverse bias, the QCSE shifts the MQW absorption edge producing modulation [Fig. 1(d_1)]. The top mirror of the SNEAM is designed in such a way that its reflectivity is as close as possible to the SNEAM cavity loss, which results in an ER as high as 10 dB around 1525 nm. Also, since the SNEAM active area diameter is of the same order of magnitude of the core of standard single-mode-fibers, light can be coupled in and out of the device with a total coupling loss of only 0.7 dB [Fig. 1(d_2)]. Furthermore, it is worth noting that, thanks to the surface-normal configuration, SNEAMs are fully transparent to the polarization state of the input light [3]. Figure 1(e) shows modulation experiments at 25 Gbit/s NRZ-OOK with excellent performance and drive voltage as low as 1 V_{pp} on the packaged SNEAM of Fig. 1(c).

3. SNEAM arrays

Thanks to their simple structure SNEAMs can be fabricated into arrays. Figure 2(a) shows a photograph of a 12-channel SNEAM array with 250 μm pitch and electrical pads in ground-signal-ground (G-S-G) configuration. Figures 2(b-c) show eye diagrams and BER curves at 25 Gbit/s for the non-packaged SNEAM array of Fig. 2(a). Eye diagrams are all well open for all the channels and, thanks to the simple SNEAM structure, a very uniform BER performance is achieved across the array, with maximum deviation of 2 dB between best and worst channels. Then, the array was butt-coupled to an AWG, and integrated on a package with RF lines and connectors, to form a multi-channel wavelength division multiplexing (WDM) transmitter [Fig. 2(d)]. The performance of the transmitter is shown in red line and square markers in Fig. 2(c), and exhibits a sensitivity penalty of less than 1 dB with respect to the worst channel of the array before packaging. It is worth noting that, the BER curve of the transmitter is measured with no active temperature control of the module. In fact, thanks to the broad wavelength range available for modulation for SNEAMs, there is no need of accurate temperature stabilization or feedback control to keep the SNEAM locked to the external laser. This result is confirmed by the measurements shown in Fig. 3, where one of the 12 channels of the non-packaged SNEAM array of Fig. 2(a) is measured versus wavelength (without optimizing the voltage conditions at each wavelength), showing a

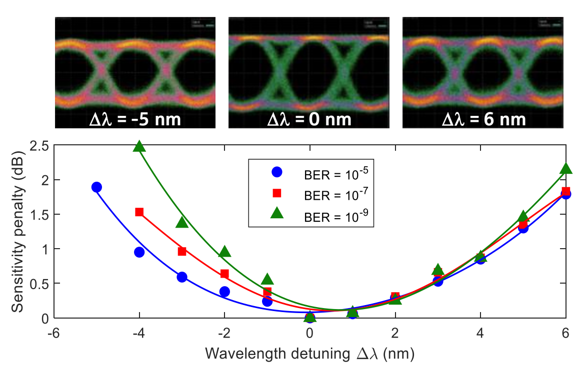

Fig. 3: Broad wavelength range available for modulation of SNEAMs (25 Gbit/s NRZ-OOK).

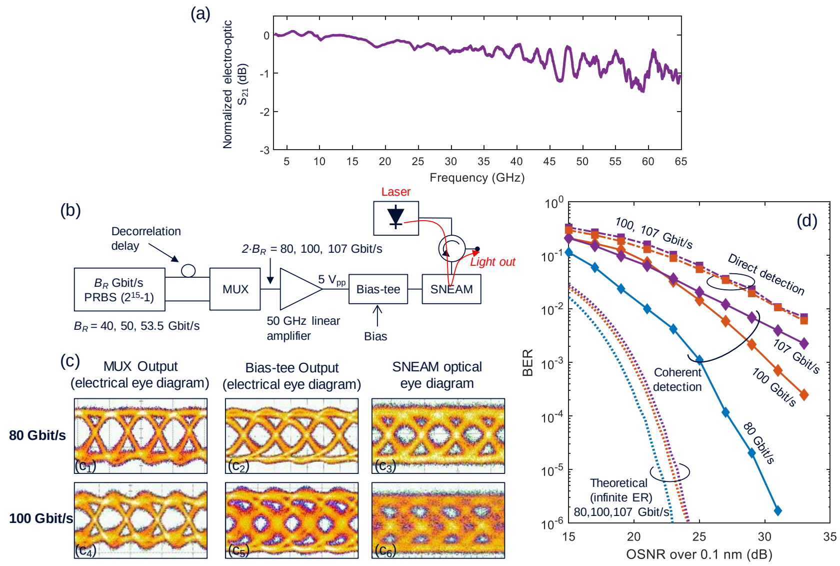

Fig. 4: (a) Electro-optic S_{21} parameter of a SNEAM. (b) Electrical setup, (c) eye diagrams and (d) BER curves at 80, 100, 107 Gbit/s NRZ-OOK. Measurements are performed with an unpackaged SNEAM.

maximum 2-2.5 dB penalty at 25 Gbit/s across more than 10 nm at different BER levels.

4. Ultra-high speed experiments

Figure 4(a) shows the electro-optic S_{21} parameter of a SNEAM with 15 μm active area diameter. The SNEAM was characterized after integration on a submount with a 50 Ohm resistor to match the impedance of the external RF cables but was not fully packaged. The measured S_{21} drops by about 1 dB across 65 GHz, suggesting that the electro-optic -3 dB bandwidth of the SNEAM is well beyond 65 GHz, the frequency limit of our setup. Modulation experiments, with bit-rate up to 107 Gbit/s, were then performed to confirm the high-speed behavior of SNEAMs [Fig. 4(b-d)]. Electrical signals at $2\cdot B_R$ = 80, 100, 107 Gbit/s were generated, using the setup shown in Fig. 4(b), by multiplexing two uncorrelated PRBSs with bit-rate B_R. The RF signal obtained is then amplified and a bias-tee combines bias voltage and RF swing before application to the SNEAM. Optical eye diagrams at the SNEAM output were measured at 80 and 100 Gbit/s [Figs. 4(c_3)-4(c_6)] with a 70 GHz photodetector and a sampling oscilloscope. The eye diagram at 80 Gbit/s [Fig. 4(c_3)] is well open and demonstrates the capability of SNEAMs to modulate at high bit-rate. A stronger distortion instead is observed at 100 Gbit/s [Fig. 4(c_6)] but, as shown by comparison of the electrical waveforms measured at the multiplexer output and after the bias-tee [Fig. 4(c_4-c_6)], it comes primarily from bandwidth limitations of the RF amplifier and of the electrical transitions between RF components, and not from the SNEAM that has sufficient bandwidth for this bit-rate. Figure 4(d) shows BER measurements versus optical OSNR. Firstly, BER was measured using a standard high-speed coherent intradyne receiver, including local oscillator, optical hybrid, high speed photodetectors, real time oscilloscope (256 GS/s, >110 GHz bandwidth), and offline DSP. Figure 4(d) shows also the theoretical BER under assumption of infinite ER and dominant ASE noise. The penalty measured at 80 Gbit/s from the theory is due to the limited ER of the modulator, with additional penalty at 100 and 107 Gbit/s due to the limited bandwidth of the electrical setup that drives the SNEAM. BER was also measured using a direct detection architecture [top of Fig. 4(d)], and exhibits a larger penalty compared to the coherent case because we cannot equalize the signal as well, since we have access only to the field amplitude.

5. Conclusion

We demonstrated SNEAM arrays with ultrawide bandwidth (>>65 GHz), ultralow coupling loss (0.7 dB) and polarization insensitive response. We showed integration of SNEAM arrays with AWGs to form WDM transmitters and modulation experiments up to 107 Gbit/s NRZ-OOK. Future integration and copackaging of SNEAM arrays with low power electronic driver chips will reduce electrical parasitics and enable high-bandwidth, low energy electro-optic engines for short-reach communication systems.

6. References

[1] C. Wang *et al.,* "Integrated lithium niobate electro-optic modulators operating at CMOS-compatible voltages," Nature 562, 101-104 (2018).
[2] J. Sun *et al.*, "A 128 Gb/s PAM4 Silicon Microring Modulator," in OFC Postdeadline Papers, OSA Technical Digest, paper Th4A.7 (2018).
[3] P. Iannone *et al.*, "44 Gb/s PAM-4 Short Reach Transmission with a Polarization-Independent Surface-Normal Electroabsorption Modulator," submitted to OFC 2020.